Entrainment of a Spatially Extended Nonlinear Structure under Selective Forcing

Michel Henriot,[1] Javier Burguete,[2,*] and Roland Ribotta[1,†]

[1]Laboratoire de Physique des Solides, Université de Paris sud, Bâtiment 510, F-91405 Orsay CEDEX, France

[2]Departamento de Física y Matemática Aplicada, Universidad de Navarra, Apartado 177, E-31080 Pamplona, Spain

(Received 7 March 2003; published 5 September 2003)

The response of a nonlinear state to a variable forcing periodic in space is studied in an extended dynamical system consisting of a liquid crystal layer driven to convection. Both the statics and the dynamics of the entrainment and the locking effects are analyzed. The dynamics of the evolution are controlled by topological singularities that allow a diffusion of the phase. The mechanisms involved are related to the role of the defects in systems undergoing spontaneous symmetry breakings.

DOI: 10.1103/PhysRevLett.91.104501 PACS numbers: 47.54.+r, 05.45.Xt, 47.20.Ky, 89.75.Kd

The properties of a dynamical system can be fully and accurately determined if, in addition to measuring the spontaneous (“natural”) response, one stimulates it by means of an appropriate external forcing. When subjected to an appropriate periodic forcing, a system with a natural periodic solution evolves as to adjust its period to the imposed one. This is the “entrainment effect” first noticed by Huyghens and studied by Van der Pol [1]. In its final state, the system is said to lock onto the forcing, or in the case of oscillators to be synchronized. Forcing has since then been applied to characterize low-dimensional systems such as mechanical, acoustic, or electrical oscillators (pacemakers) [2]. In the case of higher dimensions (pattern-forming systems), a forcing at fixed periodicity values has been used in various fields: convection [3–5], crystallization [6], Turing patterns [7], lasers [8], physiology [9], etc. By varying at will the periodicity of the forcing, one may be able to construct rapidly the stability domains of the natural states of a given spatiotemporal state and to study accurately through the dynamics, the mechanism of entrainment.

We present results on the response of a spatially extended nonlinear state of convection in a liquid crystal, forced by an external periodic pattern with variable geometry. The mechanisms and the main features of this response are also interpreted and reproduced in the frame of an appropriate Landau-Ginzburg equation.

The experimental dynamical system is the convection of a thin layer (thickness $d = 20\ \mu$m) of a nematic liquid crystal inserted between glass plates coated with semitransparent electrodes. The molecules of the nematic are made parallel to the plates (along $\vec{x}$). In the classical experiment, convection develops above some threshold in the amplitude of an ac electric field applied transversely to the layer. For the low frequency range of the ac field, well-ordered convective rolls form an almost homogeneous structure, free of defects, on very large scales L ($L \simeq 1000d$). As the amplitude is further increased, nonlinear states develop in a sequence of symmetry breakings up to the full space-time chaos [10]. The first convective state of normal rolls (NR), with wave vector $\vec{k}_0 = (k_0, 0)$ becomes unstable against the oblique rolls (OR), with wave vectors $\vec{k}_{\rm OR} = (k_x, \pm k_y)$ which break the continuous invariance along the NR axis direction $\vec{y}$. It is thus composed of two variants, i.e., domains symmetrically tilted by $\pm\theta$ over $\vec{y}$. It has been shown experimentally that, in the natural evolution of OR, only the angle changes significantly as a function of the control parameter [11]. In order to illustrate the technique in a fully nonlinear case, we shall force the angle of a spontaneous domain of this OR by coupling it to a similar external pattern with a variable angle. The coupling is realized by interposing between one electrode and the liquid crystal a photoconductive layer, on which the image of a periodic pattern is sent in monochromatic light (Fig. 1). We use a homemade layer of carbon-doped amorphous hydrogenated silicium (C-a-Si:H) 10 μm thick [12].

A mask made of a periodical array of black and transparent stripes, with period $\lambda_f = 2\pi/k_f$, is imaged on the sample by a laser source (He-Ne, 35 mW). The local electric field inside the nematic bulk is then spatially modulated in amplitude and the modulation depth is directly related to the light density on the a-Si:H layer. The spatial period of the ac field modulation is modified by varying the optical magnification of the mask image. The voltage applied on the electrodes being V_e, the forcing amplitude in the bulk is written as $V(x, y) = V_0 + \delta V \exp i(k_{f,x}x + k_{f,y}y)$. The angle of the imposed pattern

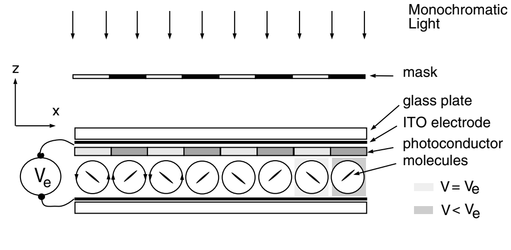

FIG. 1. Principle of forcing by an optical field spatially modulated by a mask. This field induces a spatial variation of the ac electric field in the bulk, which couples to the initial mode of convection.

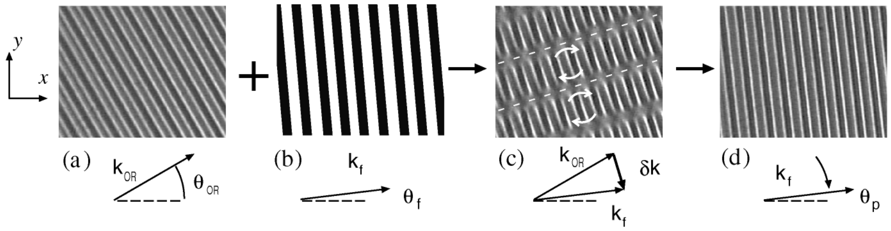

FIG. 2. Entrainment of the initial state $\vec{k}_{\rm OR}$ at angle $\theta_{\rm OR}$ (a), forced by a pattern $\vec{k}_f$ with angle θ_f (b). Periodic discommensurations are created at $|\delta k| = |\vec{k}_f - \vec{k}_{\rm OR}|$ (c) allowing a rotation (white arrows) by diffusion of the phase inside the domains between the singular lines (dashed lines), up to the uniform final state locked at $\theta_p = \theta_f$, (d).

with respect to the y axis is $\theta_f = \arctan(k_{f,y}/k_{f,x})$. In the absence of any forcing, the reduced control parameter would be $\varepsilon = (V_e^2 - V_s^2)/V_s^2$, where V_s is the threshold value. In the presence of a forcing, the global reduced constraint may be written as $\varepsilon(x, y) = \varepsilon_0 + \delta\varepsilon \exp i(k_{f,x}x + k_{f,y}y)$, where $\varepsilon_0 = (V_0^2 + \delta V^2 - V_s^2)/V_s^2$ is the mean reduced constraint, and $\delta\varepsilon = V_0\,\delta V/V_s^2$ is a measure of the modulation amplitude. The value V_0 is determined experimentally by measuring the thresholds in the absence of spatial modulation and under a calibrated homogeneous light intensity.

Now ε_0 is set slightly above threshold ($\varepsilon_0 \simeq 0.1$), and the initial state is a monodomain of one variant $\vec{k}_{\rm OR}$ at $\theta_\pm$ of the OR. The forcing wave vector will be varied by only its angle θ_f, its modulus keeping a constant value $|k_f| = |k_{\rm OR}|$. The initial OR state is here a domain of angle $\theta_{\rm OR} = -23.3°$. The initial forcing angle $\theta_f = -90°$ is incremented by steps of about 5°. The basic state remains almost stable for a large range in the forcing angle until $\theta_f \simeq -30°$ where the entrainment takes place. There, after a step has been applied, the new initial state becomes (within 0.1 sec), first, unstable against a new periodic mode of long-wavelength $\Lambda = 2\pi/\delta k$ analogous to the *beating mode* in forced oscillators, which develops an array of singular lines along the rolls axis [Fig. 2(c)]. Next, a slow rotation of the pattern of duration $\simeq 1$ sec, orients the initial state $\vec{k}_{\rm OR}$ by a phase slippage towards the direction of the forcing pattern $\vec{k}_f$. When the final angle is reached, the long-wavelength mode rapidly fades out within a short time (< 0.2 sec). This is the well-known *locking effect* [1]. After a delay of $\simeq 15$ min (much greater than any characteristic time) following each step, the forced state is in equilibrium. That final state is then used as a new initial state for the next step. The same experiment is repeated in sequence, and the resulting (the *product*) angle $\theta_p = \arctan(k_{p,y}/k_{p,x})$, where $\vec{k}_p$ is the resulting wave vector, is plotted against the forcing angle θ_f (Fig. 3). The range over which $\theta_p = \theta_f$ is the *entrainment or locking range* (Fig. 3). On both sides outside this locking range, the structure shows stationary periodic undulations which are due to simple modulation by the forcing (i.e., with period close to $|\delta k|$). The whole range, delimited by vertical dashed lines in Fig. 3, is contained inside the experimental marginal stability domain determined also by this forcing technique [12]. An additional novel effect occurs around $\theta_f = 0$, where the locking becomes suddenly ineffective. There, the final angle θ_p decreases towards the natural value θ_n (here $\theta_n \simeq 22°$)

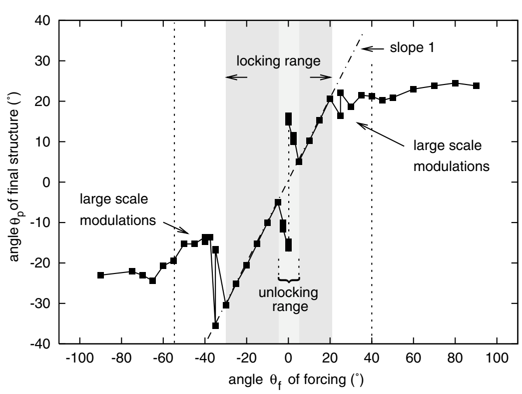

FIG. 3. Entrainment range for an initial variant $\vec{k}_{\rm OR}$ forced by $\vec{k}_f$, with $|\vec{k}_{\rm OR}| = |\vec{k}_f|$ for an amplitude $\delta\varepsilon = 0.2$ (only the angle θ_f is varied). The angle of the product state θ_p "locks" to the forcing only within a limited range (gray area). On both sides and within the dashed vertical lines, the initial state is weakly modulated. In the central part an unlocking occurs, where the two initial symmetrical variants coexist, forming a zigzag regular lattice.

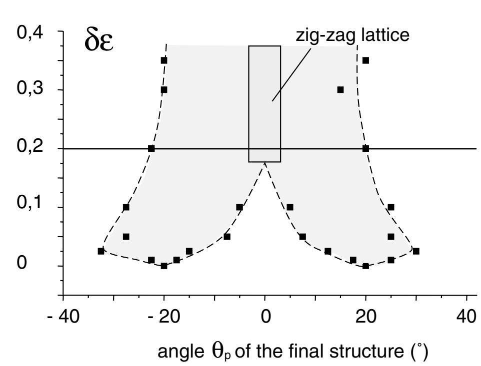

FIG. 4. Entrainment domain formed by two "locking tongues" as a function of the forcing amplitude $\delta\varepsilon$, for $\varepsilon_0 = 0.1$. Around the angle zero, the final state is the zigzag lattice made of the two initial variants, periodic along y. The horizontal dashed line corresponds to the value of $\delta\varepsilon$ used in Fig. 3.

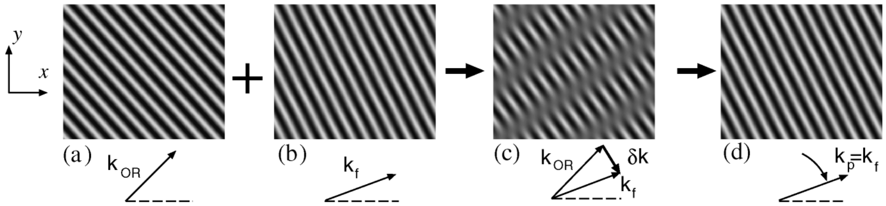

FIG. 5. Entrainment of the wave-vector direction of the initial state (a) under a spatial forcing (b) calculated by the model. The evolution is mediated by a periodic array of phase discommensurations (c), towards the uniform final state (d) as in Fig. 2.

and crosses the value zero at $\theta_f = 0$. In this small range, over 5°, the final structure is in fact a regular array made of alternate OR (zigzag), and with wave vector along y equal to $\delta k/2$. We attribute this effect to the "hidden" homogeneous mode associated with the n_y component of the director **n** specific to the OR state in a nematic [11,13], which couples to the angle θ through the n_z component. Those two n components act in an opposite way; hence, when θ_f is close to zero the high value of n_y opposes any subsequent variation of θ_p, and the forcing becomes ineffective.

By measuring the locking range for increasing values of the forcing amplitude $\delta\varepsilon$, one obtains the "locking domain" (Fig. 4) [2,14].

Because the OR state is composed of two variants, this locking domain is composed of two parts, with the typical shape of "locking tongue." It is not symmetrical here, its extension being smaller inside the $+\theta$ region. This asymmetry is due to the counteraction of the n_y homogeneous mode. In effect, in the evolution of the angle by small steps, the initial sign of the n_y mode is not inverted when the angle of the final state changes its sign. Then the final state is that of the opposite variant but with an opposite sign for n_y [12].

The starting model is a Ginzburg-Landau equation with real coefficients, of a complex envelope $A(\vec{r}) = |A| \exp(i\phi)$. The local field amplitude has the form $u(\vec{r}) = A(\vec{r}) \exp i(\vec{k}_0 \cdot \vec{r})$ [15]. The forcing at $\vec{k}_f$ with amplitude $\delta\varepsilon$ is introduced as a spatial modulation of the control parameter ε with wave vector $\vec{q}_f = \vec{k}_f - \vec{k}_0$:

$$\partial_t A = \{\varepsilon + \delta\varepsilon \exp i(\vec{q}_f \cdot \vec{r} - \phi)\}A + (\partial_x^2 + P\partial_y^2)A - \partial_y^4 A - |A|^2 A.$$

For $P \neq 1$, the model reflects the anisotropy of the system and the fourth order spatial derivative ensures a two-variant structure of OR (i.e., two symmetric orientations). In the absence of forcing and for $P > 0$, the asymptotic solution is the *Normal Rolls* state at $\vec{k} = (k_0, 0)$, i.e., $A \exp i(\vec{k}_0 \cdot \vec{x})$, and for $P < 0$, the OR appear, at $\vec{k} = \vec{k}_{\rm OR} = (\vec{k}_0 + \vec{\nabla}\phi) = (k_0, \pm\sqrt{-P/2})$. This equation has a stationary solution $A(x, y) \sim \exp i(\vec{q}_f \cdot \vec{r})$ leading to an entrained pattern at $\vec{k}_f$. The real part of the forcing term induces the beating mode at $\vec{\delta k} = \vec{k}_f - \vec{k}_{\rm OR}$. Thus, the amplitude falls down periodically and the imaginary part produces a phase excursion along periodic lines at $\vec{\delta k}$. The details of the dynamics can appear only in the numerical calculations.

We will apply the forcing only to the case $P < 0$, as in the experiment, starting from one oriented domain in the steady state ($\vec{k}_{\rm OR}$) obtained for $\delta\varepsilon = 0$. The calculations are made with periodic boundary conditions, using a finite-difference scheme of fifth order in space to account more accurately for the large space gradients, and a semi-implicit scheme of order five in time. At fixed values of ε and $\delta\varepsilon$, a wave vector $\vec{k}_f$ is applied and the resulting state $\vec{k}_p$ is measured. The asymptotic final state is reached (within a 2% error) typically after ten time units for $\delta\varepsilon \sim 0.3$ (10^5 steps). The evolution is here quite similar to the experimental one: The large phase gradients present along the periodic lines turn into linear singularities in the phase. Those lines separate domains (domain walls) inside which a slow rotation occurs to change the local wave vector (Fig. 5) and fade out when the final angle is reached (locking).

By varying the forcing angle θ_f, one obtains the entrainment for the basic structure over the stability domain of the OR. The result (Fig. 6) shows the *locking range* where $\vec{k}_p = \vec{k}_f$, with a sharp border separating it from the unlocked state $\vec{k}_p = \vec{k}_0$. This locking range is symmetrical with respect to $\theta_f = 0$, because the model does not include the "hidden symmetry." The same experiment is repeated for different values of the modulation amplitude $\delta\varepsilon$, and for two sets of angles $\pm\theta_f$ in

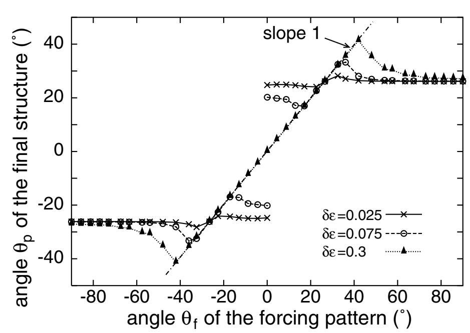

FIG. 6. Numerical range of entrainment for $\varepsilon = -0.05$, $\delta\varepsilon = 0.025$ 0.075, 0.3. Along the oblique line $\theta_p = \theta_f$. The $\delta\varepsilon = 0.3$ case is similar to that of Fig. 3. The initial angle is $\theta_i = 26°$.

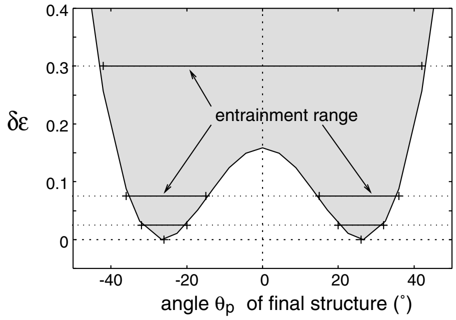

FIG. 7. Entrainment domains obtained numerically as a function of the forcing amplitude $\delta\varepsilon$, for $\varepsilon = -0.05$. The horizontal lines refer to the values $\delta\varepsilon$ used in Fig. 6.

order to calculate the locking domains. Figure 7 shows the overlapping of the two locking domains as in the experiment.

Both the experiment and the calculations show that, under a selective forcing, a basic state may be entrained, and within a limited range the initial pattern is locked to the imposed state. The entrainment is realized in space by two mechanisms acting in sequence. First, a new transient mode due to the lowest order nonlinearities (beating) superimposes on the basic state, producing an array of topological singularities of the phase (domain walls) at $|\delta k| = |\vec{k}_f - \vec{k}_{\rm OR}|$ which are in fact discommensurations [4]. Second, inside the enclosed domains separated by those lines at $\Lambda = 2\pi/\delta k$, the phase rotates by a slow diffusion. As the system is relaxational, this diffusion takes place over times varying as Λ^2. Here, the duration time is $\tau_d \sim 1/|\delta q|^2$ and it diverges when $|\delta q|$ approaches zero (case of homogeneous states). Once the final state is reached, the whole forcing constraint is relaxed and the transient beating mode disappears.

Because the forcing mode is coherent, the splitting of the basic structure in multidomains is regular. In heterogeneous structures, sidebands of the basic mode may be nonlinearly excited thus creating at random transient domains with different wave vectors, involving dislocations and domains walls. The walls, being topologically analogous to the discommensurations, play the same role [16], and then the transformations under a sudden and large increase of the control parameter occur rapidly (the most frequent case). This process is also facilitated by the large scale modulations often present at random in space in any spatially extended system [11]. Thus, the multidomain formation allows the transformation to occur by diffusion within times much shorter than in ideal homogeneous symmetry breakings. Usually, pattern formation is rather achieved in this way (defect-mediated transformations) [17]. Other examples are the Eckhaus instability and the defect-mediated chaos. Hence, these results may help in interpreting the intricate transient structures and the role of the defects in the symmetry breakings occurring in an extended dynamical system, when the control parameter is suddenly varied. This double mechanism of structure evolution is very similar to the *martensitic transformation* in crystalline solids [18].

We have shown how selective forcing provides an efficient tool to study and even control the main properties of extended nonlinear systems. It is found that the dynamics of the entrainment involves a double mechanism of creation of small domains mediated by singularities, allowing a rapid change of the wave vector by diffusion of the phase. These results show the decisive action of the defects and they should apply as well in other highly dimensional systems undergoing structure transformations.

We thank Pierre Lallemand for inviting one of us (J. B.) to the Orsay ASCI/CNRS laboratory and we thank the MCyT of the Spanish Government for support (Project No. BFM2002-02011).

*Electronic address: javier@fisica.unav.es
†Electronic address: ribotta@lps.u-psud.fr

[1] B. Van der Pol, Philos. Mag. **3**, 65 (1927).
[2] N. Minorsky, *Introduction to Non-Linear Mechanics* (J.W. Edwards, Ann Arbor, 1947).
[3] F. H. Busse and J. A. Whitehead, J. Fluid Mech. **47**, 305 (1971).
[4] M. Lowe and J. P. Gollub, Phys. Rev. Lett. **51**, 786 (1983).
[5] D. Semwogerere and M. F. Schatz, Phys. Rev. Lett. **88**, 054501 (2002).
[6] L. M. Williams, M. Muschol, X. Qian, W. Losert, and H. Z. Cummins, Phys. Rev. E **48**, 489 (1993).
[7] S. Rüdiger, D. G. Míguez, A. P. Muñuzuri, F. Sagués, and J. Casademunt, Phys. Rev. Lett. **90**, 128301 (2003).
[8] T. Sugawara, M. Tachikawa, T. Tsukamoto, and T. Shimizu, Phys. Rev. Lett. **72**, 3502 (1994).
[9] S. R. Cobb, E. H. Buhl, K. Halasy, O. Paulsen, and P. Somogyi, Nature (London) **378**, 75 (1995).
[10] A. Joets and R. Ribotta, J. Phys. (Paris) **47**, 595 (1986).
[11] A. Belaidi, Ph.D. thesis, Université Paris-sud, Orsay, 1998.
[12] M. Henriot, Ph.D. thesis, Université Paris-sud, Orsay, 2001.
[13] E. Plaut, W. Decker, W. Pesch, A. Rossberg, L. Kramer, A. Belaidi, and R. Ribotta, Phys. Rev. Lett. **79**, 2367 (1997).
[14] A. Andronov and A. Witt, Arch. Elektrotek. **24**, 99 (1930).
[15] W. Pesch and L. Kramer, Z. Phys. B **63**, 121 (1986).
[16] A. Joets and R. Ribotta, J. Stat. Phys. **64**, 981 (1991).
[17] R. Ribotta, in *Nonlinear Phenomena in Materials Science*, edited by L. Kubin and G. Martin (Trans Tech Publications, Switzerland, 1988).
[18] J.W. Christian, *The Theory of Transformations in Metals and Alloys* (Pergamon, Oxford, 1965).